

Growth of stoichiometric (002) ZnO thin films on Si (001) substrate by using plasma enhanced chemical vapor deposition

B. S. Li, Y. C. Liu, Z. Z. Zhi, D. Z. Shen, J. Y. Zhang et al.

Citation: *J. Vac. Sci. Technol. A* **20**, 1779 (2002); doi: 10.1116/1.1503783

View online: <http://dx.doi.org/10.1116/1.1503783>

View Table of Contents: <http://avspublications.org/resource/1/JVTAD6/v20/i5>

Published by the AVS: Science & Technology of Materials, Interfaces, and Processing

Related Articles

Substrate-biasing during plasma-assisted atomic layer deposition to tailor metal-oxide thin film growth

J. Vac. Sci. Technol. A **31**, 01A106 (2013)

Substrate temperature and electron fluence effects on metallic films created by electron beam induced deposition

J. Vac. Sci. Technol. B **30**, 051805 (2012)

Effect of O₂ gas partial pressure on mechanical properties of Al₂O₃ films deposited by inductively coupled plasma-assisted radio frequency magnetron sputtering

J. Vac. Sci. Technol. A **30**, 051511 (2012)

Tetragonal or monoclinic ZrO₂ thin films from Zr-based glassy templates

J. Vac. Sci. Technol. A **30**, 051510 (2012)

Phase identification and control of thin films deposited by co-evaporation of elemental Cu, Zn, Sn, and Se

J. Vac. Sci. Technol. A **30**, 051201 (2012)

Additional information on *J. Vac. Sci. Technol. A*


Journal Homepage: <http://avspublications.org/jvsta>

Journal Information: http://avspublications.org/jvsta/about/about_the_journal

Top downloads: http://avspublications.org/jvsta/top_20_most_downloaded

Information for Authors: http://avspublications.org/jvsta/authors/information_for_contributors

ADVERTISEMENT




Aluminum Valves with Conflat® Flanges

Less Outgassing Than Stainless
Mate to Stainless Steel Conflats
Sizes From 2.75 to 14 inch O.D.
Leak Rate Less Than 10^{-10} SCC/S

Visit us
at Booth # 300
in Tampa

Prices & Specifications
vacuumresearch.com



Growth of stoichiometric (002) ZnO thin films on Si (001) substrate by using plasma enhanced chemical vapor deposition

B. S. Li and Y. C. Liu^{a)}

Open Laboratory of Excited State Processes, Chinese Academy of Sciences and Changchun Institute of Optics, Fine Mechanics and Physics, Chinese Academy of Sciences, 1-Yan An Road, Changchun 130021, People's Republic of China

Z. Z. Zhi

Institute of Theoretical Physics, Northeast Normal University, Changchun 130024, People's Republic of China

D. Z. Shen, J. Y. Zhang, Y. M. Lu, X. W. Fan, and X. G. Kong

Open Laboratory of Excited State Processes, Chinese Academy of Sciences and Changchun Institute of Optics, Fine Mechanics and Physics, Chinese Academy of Sciences, 1-Yan An Road, Changchun 130021, People's Republic of China

(Received 13 December 2001; accepted 8 July 2002)

ZnO thin films have been grown on Si(100) substrate by plasma enhanced chemical vapor deposition using a zinc organic source $[\text{Zn}(\text{C}_2\text{H}_5)_2]$ and carbon dioxide (CO_2) gas mixture at 503 K. The dependence of ZnO thin film quality on the gas flow rate ratio of $\text{Zn}(\text{C}_2\text{H}_5)_2$ to CO_2 (GFRRZC) is studied by x-ray diffraction (XRD), optical absorption (OA) spectra, and photoluminescence (PL) spectra. An excitonic absorption peak is observed in the OA spectra, which closely depends on the GFRRZCs. The XRD spectra show that a *c*-axis-orientated wurtzite structure ZnO thin film with the full width at half maximum (FWHM) of 0.24° has been prepared. The PL spectra show a strong UV emission with a narrow FWHM of 105 meV at 3.289 eV with a weak deep-level defect emission around 2.5 eV, implying the formation of the stoichiometric ZnO thin films. The origin of the UV band is from the free exciton recombination testified by the temperature dependent PL spectra. © 2002 American Vacuum Society. [DOI: 10.1116/1.1503783]

I. INTRODUCTION

ZnO, one of those important semiconductors with many attractive features, has versatile physical properties such as piezoelectrical, ferroelectrical, electro-optical, acousto-optical, and luminescence characteristics. ZnO has been applied in many fields. Recently, ZnO had exerted a strong fascination upon scientists and became a hotspot in a wide band gap semiconductor, in particular, Service reported its potential application in UV laser diode.¹ Optically pumped stimulated emission and lasing of ZnO have already been demonstrated.^{2–4} Furthermore, ZnO device does not suffer from dislocation degradation during its operation as it is one of the “hardest” material in the II–VI compound family. And it is also much more stable to resist radiation damage than other common semiconductors. Generally, it is accepted that ZnO is the most promising material for realizing an UV laser at room temperature. This is because ZnO has a wide band gap of 3.3 eV with a large exciton binding energy of 60 meV.

In those exciting researches on the photoluminescence (PL) of ZnO thin films, the samples were grown on Al_2O_3 , ScAlMgO_4 , or MgAl_2O_4 substrates.^{2–8} Recently, some researchers have prepared ZnO thin films on Si substrate by radical source molecular-beam epitaxy (MBE).⁹ In this ar-

ticle, stoichiometric ZnO thin films with *c*-axis orientation were prepared by employing the plasma enhanced chemical vapor deposition (PECVD) using a zinc organic source $[\text{Zn}(\text{C}_2\text{H}_5)_2]$ and carbon dioxide (CO_2) gas mixtures at a low temperature of 503 K. In terms of our knowledge, there are few papers on ZnO thin films prepared on Si substrate by PECVD with good luminescence properties.

A set of samples was prepared to investigate the formation mechanism of *c*-axis-oriented ZnO thin film. The properties of the ZnO thin films are studied employing x-ray diffraction (XRD), optical absorption spectra (OA), and PL spectra. The UV band comes from free exciton recombination, which is testified by the temperature dependent PL spectra.

II. EXPERIMENTAL PROCEDURE

ZnO thin films are grown by PECVD from the gas mixture of diethylzinc and carbon dioxide. The schematic structure of the PECVD system has been introduced elsewhere,¹⁰ which has the 15-cm-diameter parallel-faced electrodes for the capacitive coupling discharge. The chamber size is 22 cm in diameter and 21 cm in height. The electrode spacing is 3 cm, and the discharge is observed as almost uniform throughout the 15-cm-diameter electrode area. The diethylzinc source is operated in a bath kept refrigerated at 6°C by a continuous wave-1 type fine controlled temperature semiconductor device, and is carried into the chamber by bubbling gas of high-purity H_2 . The experimental procedure and

^{a)} Author to whom correspondence should be addressed. Also at Institute of Theoretical Physics, Northeast Normal University, Changchun 130024, P. R. China; electronic mail: ycliu@nenu.edu.cn

TABLE I. The deposition conditions of ZnO thin films with changing the GFRRZC.

Sample	GFRRZC	(rf) power (W)	Temperature of the substrate (K)	Gas flow rate of argon (sccm)
A	4:2	35	503	8
B	4:4	35	503	8
C	4:5	35	503	8
D	4:6	35	503	8
E	4:7	35	503	8

the parameters had been introduced in detail previously.¹⁰ A series of samples has been grown on Si substrates with different gas flow ratio rate of $\text{Zn}(\text{C}_2\text{H}_5)_2$ to CO_2 (GFRRZC). The pressure in the chamber varied from 110–130 Pa during the GFRRZC experiment. The detailed growth conditions are listed in Table I.

The crystalline quality of the ZnO layers was examined by XRD using a rotating anode x-ray diffractometer with $\text{Cu } K\alpha_1$ radiation of 1.54 Å. The OA spectra were measured by an UV-360 Recording Spectrophotometer (Shimadzu) at room temperature. A deuterium lamp was the light source with the wavelength range of 200 to 460 nm. The signals were detected by a R_{456} -type photoelectric multiplier with a high resolution of 0.1 nm. The PL spectra were measured using an UV Labran Infinity Spectrophotometer (J-Y Company, French) excited by a continuous He–Cd laser with 30 mW and detected by a charge coupled device camera with a high resolution of 0.04 nm. The temperature dependent PL spectra are obtained using the 325 nm line of a He–Cd laser and a PL microprobe measurement system (J-Y company, French). Measurements below room temperature were taken in the range of 83 to 458 K by placing the sample cells in a cryogenic unit.

III. RESULTS AND DISCUSSION

Figures 1(a)–1(e) show the XRD spectra of the ZnO thin films prepared at a substrate temperature of 503 K by using PECVD with different GFRRZC. It is clear from the XRD data that the ZnO thin films were all *c*-axis (002) orientation. Only the weak peaks of (100), and (103) appear when the GFRRZC is 4:2, as shown in Fig. 1(a). However, the orientation of ZnO thin film is dependent on GFRRZC at lower temperature of 453 K.¹⁰ To investigate the dependence of orientation of ZnO thin films on the substrate temperature, a series of samples F to I were prepared at different temperatures with same deposition conditions as sample C. The substrate temperatures were 373, 413, 443, and 503 K, respectively. The evolution of the (002) preferred orientation was examined by XRD, as shown in Fig. 2. At a low substrate temperature, the ZnO thin films are polycrystalline with different orientations, as shown in Figs. 2(f) and 2(g). When the growth temperature reaches 443 K, the diffraction peak of (002) ZnO makes a dramatic increase. A preferred orientation of (002) is realized for the growth temperature of 503 K, as shown in Fig. 2(i). The dependence of the film quality on

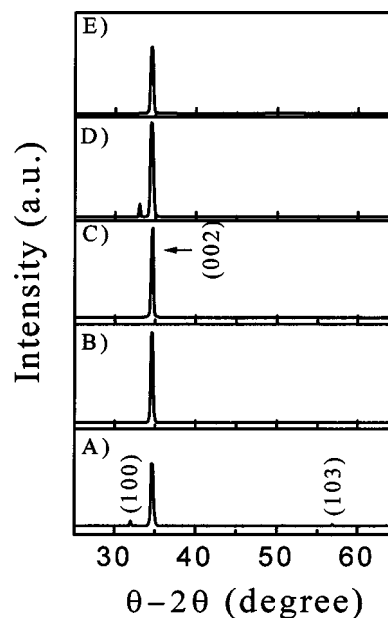


FIG. 1. XRD patterns of the ZnO thin films grown on Si(100) substrates under the different GFRRZCs: (a) 4:2, (b) 4:4, (c) 4:5, (d) 4:6, and (e) 4:7.

substrate temperature can be interpreted by the mobility and diffusion of the reactants on the substrate surface. At low temperature, the radicals with low surface mobility will be located at different positions within the substrate due to the lack of thermal activated energy. Thus, the initial crystal nucleus tends to grow in the direction of available reactant flux, leading to different orientations of crystal grains and the formation of polycrystalline films. As the substrate temperature increases, the mobility of reactants increases. It is well known that the surface free energy of semiconductors

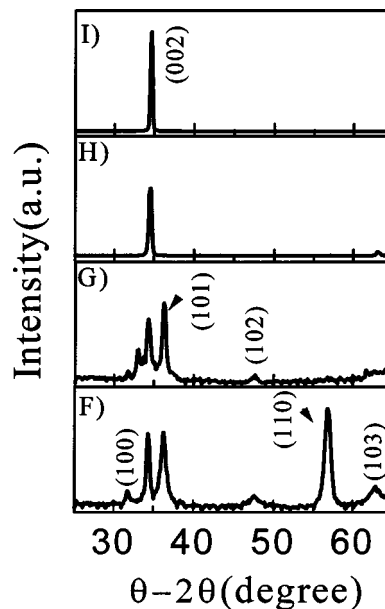


FIG. 2. XRD spectra of the ZnO thin films prepared by PECVD with a fixed GFRRZC of 4:5 under the different substrate temperature: (f) 373 K, (g) 413 K, (h) 443 K, and (i) 503 K.

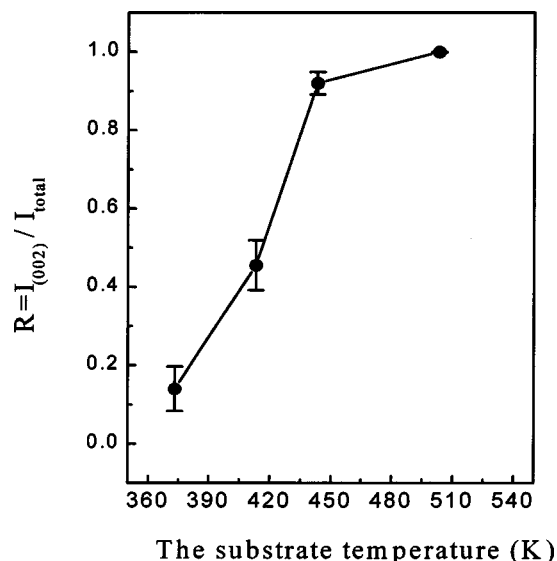


FIG. 3. Dependence of the diffraction intensity ratio of the ZnO (002) peak to all the peaks on the substrate temperature, $R = I_{(002)} / I_{\text{total}}$.

strongly depends on the hybridized orbit. For the materials with a sp^3 hybridized orbit, which is the most important bonding style among the $A^N B^{N-8}$ type semiconductors, each directed orbit spread along the [111] direction in the cubic structure, and along the [002] direction in hexagonal structure. When the film was deposited onto a substrate without the influence of epitaxy, the surface of a film tends to be either the (111) or the (002) plane, because these planes have minimum surface free energies.¹¹ Of course, this model is appropriate for the case where the atomic diffusion is large at the surface of the growing film.¹² The substrate temperature is an important factor to effect the surface mobility of the atomic for supplying the thermal energy to the species that are absorbed on the surface of the substrate. When the temperature of the substrate is raised to 503 K, the mobility of the adsorbed species is large enough to form an ordered ZnO thin film. Thus, all samples show the (002) preferred orientation.

The relative number of crystal oriented in a certain direction could be related to the area of the XRD peak, representing that reflection. Thus, the ratio of the diffraction intensity of the (002) ZnO peak to all the peaks was defined:

$$R = I_{(002)} / I_{\text{total}},$$

where the $I_{(002)}$ and I_{total} are the diffraction intensity of (002) peak and the total of all the peak, respectively. Which were plotted as a function of the growth temperature as shown in Fig. 3. It is noted the fact that to realize a c -axis-oriented ZnO thin film needs a much lower temperature by using PECVD than other techniques. Because a lot of high-energy particles in plasma would collide with the atoms that were adsorbed in the surface and exchange the momentum each other, the mobility of the atoms was enhanced,¹³ which is favorable to form a c -axis-oriented ZnO thin films at low substrate temperature.

Figure 4 shows the absorption spectra for samples A to E

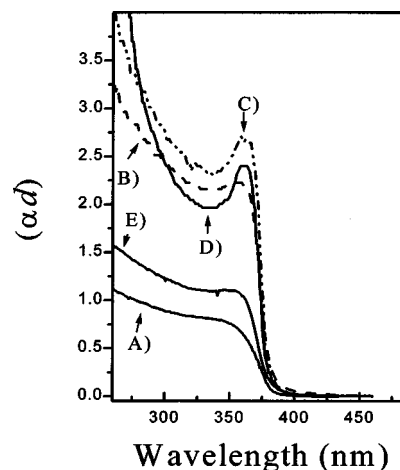


FIG. 4. Optical absorption spectra of ZnO thin films grown under different GFRRZCs. (a) 4:2, (b) 4:3, (c) 4:5, (d) 4:6, and (e) 4:7.

at room temperature. The character of absorption spectra is closely dependent on the GFRRZC. At the optimizing GFRRZC, such as samples C and D, an obvious absorption peak of the free exciton is observed near the absorption edge.^{14,15} Generally, the exciton with a small binding energy in semiconductor only exists at low temperature. However, the exciton absorption in ZnO can be observed at room temperature, and above, due to its large binding energy of 60 meV. Thus, the absorption spectra of ZnO films display an exciton effect. Usually, the effect of exciton in semiconductor is not only dependent on its binding energy, but also on its crystal quality. The exciton will not exist due to additional scattering by impurities and defects.¹⁶ For example, there is a very weak exciton absorption peak in OA spectra of samples A and E. Figure 4 suggests that high-quality ZnO films have been prepared when the GFRRZC is fixed at 4:5 and 4:6. The onset energy position of the absorption can be obtained by extrapolating $(\alpha h\nu)^2$ against $h\nu$ to zero,¹⁷ where α is the absorption coefficient and $h\nu$ is the photon energy. The absorption edges for the five samples are then obtained as 3.286, 3.289, 3.297, 3.300, and 3.301 eV, respectively. These values are in excellent agreement with the absorption edge of the bulk ZnO (3.3 eV),¹⁸ indicating that the quality of ZnO thin films improved at the optimizing GFRRZC.

Figure 5 shows the PL spectra of the ZnO thin films measured at room temperature. For the PL spectra, the main emission properties were closely dependent on the GFRRZCs. The UV band was assigned to be the free exciton recombination,^{19,20} which will be testified by the temperature dependent PL spectra in the next section. The full width at half maximums (FWHMs) of the PL spectra of samples A–E are 160, 154, 147, 105, and 133 meV, respectively. The line-width measured at room temperature is 105 meV which should be compared with 120 meV,²¹ 117 meV,²² and 109 meV (Ref. 23) which have been reported. There is a blueshift from 3.238 to 3.289 eV in the UV emission position of the PL spectra, as shown in Fig. 5. Between the PL spectra and the optical absorption edge, the Stokes shift of samples A to E are 47, 34, 34, 11, and 28 meV. In general, electron–

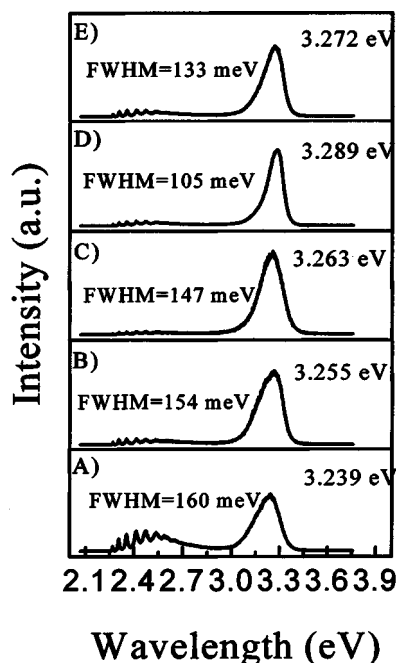


FIG. 5. PL spectra of ZnO thin films prepared at low temperature of 503 K with different GFRRZCs: (a) 4:2, (b) 4:4, (c) 4:5, (d) 4:6, and (e) 4:7.

phonon coupling, lattice distortions, localization of charge carriers due to interface defects or point defects may cause the redshift of emission line from the absorption edge.¹⁴ The decreasing of the Stokes shift from 47 to 11 meV may be due to the defect reduction. Generally, the UV band was overlapped by the free exciton and binding exciton located by the defects at room temperature. With ZnO thin-film quality improved, the density of defects was reduced, resulting in a narrower FWHM as well as a blueshift in the UV band. The deep-level emission band around 2.5 eV was strongly dependent on the supplied CO₂. It is accepted that the green band is associated with oxygen vacancies (V_O).²⁴ A lot of V_O will be produced at deficient CO₂ supplied, that is the lack of activated oxygen. One way to evaluate the concentration of structural defects in ZnO is to compare the relative PL intensity ratio of the UV band to the deep-level green emission. The reported PL spectra of ZnO power or polycrystalline thin films have shown much stronger deep-level emission than UV emission, resulting in a relative PL intensity ratio of near zero at room temperature. The epitaxial thin films grown by metalorganic chemical vapor deposition and MBE show relatively weaker deep-level emission, in the ratio of 1 and 20, respectively, at room temperature due to the reduced structure defects.^{22,25} In our results, the ratios of UV band to visible emission were 3, 18, 40, 27, and 14, respectively. The structure defects of the ZnO thin films were reduced further. There is an interesting result in the PL spectra. With the increasing of the CO₂ supplied, the ratio of the UV band to the visible band increase at first then decrease, as shown in Fig. 5. Maybe it was that the excess oxygen atoms recombine O₂, in fact causing the lack of the active oxygen. It is well known that the binding energy of an oxygen molecule is 5.16 eV, and it is difficult to break O₂ into active oxygen

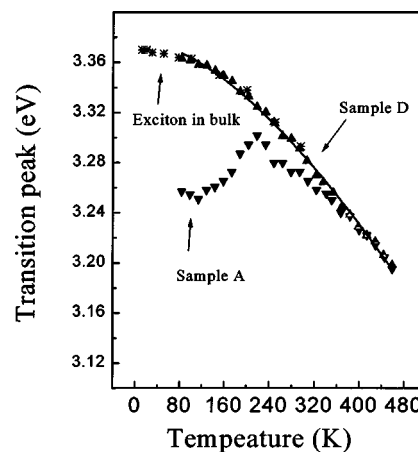


FIG. 6. Temperature dependence of the peak energy for sample A (up triangle) and sample D (down triangle) in the UV emission. The stars show the temperature dependence of free exciton in bulk ZnO (Ref. 16) for comparison. The down triangle data points are experimental points simulated by the theoretical formula, equation $E_g = E_0 - \alpha T^2 / (T + \beta)$.

atoms, causing many oxygen vacancies in ZnO thin films prepared by a conventional method. Even at higher active oxygen concentration, V_O defects readily form due to its low formation energy, which are supported by a first-principle calculation.^{26,27} Thus, a low growth temperature is crucial to decrease the V_O defects. In our experiment, the ZnO thin films are formed in the plasmas at low growth temperature. The reactive zinc ions or atoms react directly with active oxygen ions or atoms obtained from CO₂ decomposed by plasma. As a result, it is easy to obtain stoichiometric films.

There are slight differences in the UV band of samples with different GFRRZCs. The origins of them may result from different mechanisms. The temperature dependent PL spectra of samples A and D are measured to investigate the origins. It is well known that the variation in the energy gap with temperature is due to a shift in the relative position of the conduction and valence bands.²⁸ The peak of transition energy of both samples A (up triangle) and D (down triangle) are plotted against temperature, as shown in Fig. 6. The free exciton in bulk (the stars) that depends on temperature is also plotted for comparison. The peak of transition energy of sample D is a good coincidence with exciton position in bulk,¹⁴ as shown in Fig. 6, meaning the origin of UV band in sample D is from the recombination of the free exciton. The transition energy position of an exciton in sample D is simulated by Varshini's empirical function as²⁸

$$E_g(T) = E_g(0) - \alpha T^2 / (T + \beta), \quad (1)$$

where $E_g(0)$, α , and β are fitting parameters. The obtained α , β , and $E_g(0)$ are 9.5×10^{-4} eV/K, 644 K, and 3.376 eV, respectively. The obtained energy position at 0 K, $E_g(0) = 3.376$ eV, also agrees quite well with the reported values for the energy position of the free exciton in ZnO.^{29,30} Contrary to sample D, sample A, which was prepared at the lowest flow of CO₂, shows anomalous optical properties as shown in Fig. 6 (down triangle). The transition energy of sample A increased with increasing temperature in the range

of 83 to 218 K. Then, the transition energy of sample A is smaller than sample D from 218 to 365 K. Above 365 K, the peak position of transition energy of samples A and D is equal. Such an anomalous temperature dependence is probably because of the localized states forming excitons. The more defect density there is, the more localized excitons. At a low temperature, the binding excitons mainly contribute to the luminescence since excitons do not have enough thermal energy to be activated. As the temperature is increased, the energy peak shifts to the low-energy side due to the decreasing of the band gap. A further increase in temperature causes the binding exciton localized by the defects to become free exciton, resulting in enhanced emission from the free exciton. Therefore, the total peak energy shifts to the high-energy side. At the interim of temperature, emission is overlapped from the binding excitons and free excitons, causing the lower energy in sample A than that in sample D. By further increasing the temperature, the binding excitons are fully activated into free excitons. As a result, the transition energy of the sample A shows the same as the sample D with increasing temperature.

IV. CONCLUSION

The *c*-axis-oriented ZnO thin films were prepared by PECVD from the gas mixture of diethylzinc and carbon dioxide at a low temperature (503 K). The mobility of the surface atoms plays an important role in the formation of the preferred oriented thin films, and testified at various substrate temperatures. A pronounced exciton peak was observed in the absorbed spectra. Improved UV emission from free exciton recombination was obtained with high ratio of the UV band to the deep-level green emission, implying the formation of stoichiometric ZnO thin films. Supplying enough activated oxygen and a low growth temperature are both key to the formation of stoichiometric ZnO thin films.

ACKNOWLEDGMENTS

This work was supported by the Program of CAS Hundred Talents, the National Fundamental and Applied Research Project, the Key Project of the National Natural Science Foundation of China No. 69896260, the National Natural Science Foundation of China, the Innovation Foundation of CIOFP, Excellent Young Teacher Foundation of Ministry of Education of China, and Jilin Distinguished Young Scholar Program.

- ¹R. F. Service, *Science* **276**, 895 (1997).
- ²P. Yu, Z. K. Tang, G. K. L. Wong, M. Kawasaki, A. Ohtomo, and H. Koinuma, *J. Cryst. Growth* **184**, 601 (1998).
- ³Y. F. Chen, D. M. Bagnall, Z. Q. Zhu, T. Sekiuchi, K. Park, K. Hiraga, T. Yao, S. Koyama, M. Y. Shen, and T. Goto, *J. Cryst. Growth* **181**, 165 (1997).
- ⁴M. H. Huang, S. Mao, H. Feick, H. Yan, Y. Y. Wu, H. Kind, E. Weber, R. Russo, and P. Yang, *Science* **292**, 1897 (2001).
- ⁵Y. F. Chen, N. T. Tuan, Y. Segawa, H. Ko, S. Hong, and T. Yao, *Appl. Phys. Lett.* **78**, 1469 (2001).
- ⁶K. K. Kim, J. H. Song, H. J. Jung, S. J. Park, J. Song, and J. Y. Li, *J. Vac. Sci. Technol. A* **18**, 2864 (2000).
- ⁷T. Makino, C. H. Chia, N. T. Tuan, Y. Segawa, M. Kawasaki, A. Ohtomo, K. Tamura, and H. Koinuma, *Appl. Phys. Lett.* **76**, 3549 (2000).
- ⁸Y. F. Chen, S. Hong, H. Ko, M. Nakajima, T. Yao, and Y. Segawa, *Appl. Phys. Lett.* **76**, 245 (2000).
- ⁹K. Iwata, P. Fons, S. Niki, A. Yamada, K. Matsubara, K. Nakahara, T. Tanabe, and H. Takasu, *J. Cryst. Growth* **214**, 50 (2000).
- ¹⁰B. S. Li, Y. C. Liu, D. Z. Shen, Y. M. Lu, J. Y. Zhang, X. G. Kong, X. W. Fan, and Z. Z. Zhi, *J. Vac. Sci. Technol. A* **20**, 265 (2002).
- ¹¹N. Fujinura, T. Nishihara, S. Goto, J. F. Xu, and T. Ito, *J. Cryst. Growth* **130**, 269 (1993).
- ¹²G. Knuyt, C. Quaeys, J. D'Haen, and L. M. Stals, *Thin Solid Films* **258**, 159 (1995).
- ¹³Y. J. Kim and H. J. Kim, *Mater. Lett.* **21**, 351 (1994).
- ¹⁴C. L. Yang, J. N. Wang, W. K. Ge, L. Guo, S. H. Yang, and D. Z. Shen, *J. Appl. Phys.* **90**, 4489 (2001).
- ¹⁵Z. K. Tang, G. K. L. Wong, P. Yu, M. Kawasaki, A. Ohtomo, H. Koinuma, and Y. Segawa, *Appl. Phys. Lett.* **72**, 3270 (1998).
- ¹⁶H. J. Ko, Y. F. Chen, Z. Zhu, T. Yao, I. Kobayashi, and H. Uchiki, *Appl. Phys. Lett.* **76**, 1905 (2000).
- ¹⁷V. Srikant and D. R. Clarke, *J. Appl. Phys.* **81**, 6357 (1997).
- ¹⁸V. Srikant and D. R. Clarke, *J. Appl. Phys.* **83**, 5447 (1998).
- ¹⁹K. K. Kim, J. H. Song, H. J. Jung, S. J. Park, J. H. Song, and J. Y. Lee, *J. Vac. Sci. Technol. A* **18**, 2864 (2000).
- ²⁰T. V. Butkhuzi, T. G. Chelidze, A. N. Georgobiani, D. L. Jashiasvili, T. G. Khulordava, and B. E. Tsekvava, *Phys. Rev. B* **58**, 10692 (1998).
- ²¹A. B. M. Almamun Ashrafi, A. Ueta, A. Avramescu, H. Kumano, Y. W. Ok, and T. Y. Seong, *Appl. Phys. Lett.* **76**, 550 (2000).
- ²²Y. F. Chen, D. M. Bagnall, H. J. Ko, K. T. Park, Z. Zhu, and T. Yao, *J. Appl. Phys.* **84**, 3912 (1998).
- ²³M. A. L. Johnson, S. Fugita, W. H. Rowland, Jr., W. C. Hughes, J. W. Cook, Jr., and J. F. Schetzina, *J. Electron. Mater.* **25**, 855 (1996).
- ²⁴K. Vanheusden, W. L. Warren, C. H. Seager, D. R. Tallant, J. A. Voigt, and B. E. Gnade, *J. Appl. Phys.* **79**, 7983 (1996).
- ²⁵S. Bethke, H. Pan, and B. W. Wessels, *Appl. Phys. Lett.* **52**, 138 (1988).
- ²⁶Y. Yan, S. B. Zhang, S. B. Pennycook, and S. T. Pantelides (unpublished).
- ²⁷S. B. Zhang, S. H. Wei, and A. Zunger, *Phys. Rev. B* **63**, 075205 (2001).
- ²⁸Y. P. Varshni, *Physica (Amsterdam)* **34**, 149 (1967).
- ²⁹W. Y. Liang and A. D. Yoffe, *Phys. Rev. Lett.* **20**, 59 (1968).
- ³⁰D. G. Thomas, *J. Phys. Chem. Solids* **15**, 86 (1960).